Research Square

Preprints are preliminary reports that have not undergone peer review.
They should not be considered conclusive, used to inform clinical practice,
or referenced by the media as validated information.

Herbivore-induced shifts in volatile organic compounds and phytohormone crosstalk are associated with Asian longhorned beetle aggregation on Russian olive

Xinrui Zhao
Beijing Forestry University
Yaoxiang Lei
Beijing Forestry University
Chengcheng Li
Beijing Forestry University
Min Liu
Beijing Forestry University
Jiale Li
Hunan Academy of Forestry
Shixiang Zong
Beijing Forestry University
Lili Ren
lily_ren@bjfu.edu.cn

Beijing Forestry University
Youqing Luo
Beijing Forestry University

Research Article

Keywords: Anoplophora glabripennis, Elaeagnus angustifolia L., dead-end trap tree, HIPVs, phytohormones

Posted Date: November 19th, 2026

DOI: https://doi.org/10.21203/rs.3.rs-11540768/v1

License: This work is licensed under a Creative Commons Attribution 4.0 International License.
Read Full License

Additional Declarations: No competing interests reported.

Herbivore-induced shifts in volatile organic compounds and phytohormone crosstalk are associated with Asian longhorned beetle aggregation on Russian olive

Authors: Xinrui Zhao[1], Yaoxiang Lei[1], Chengcheng Li[1], Min Liu[1], Jiale Li[2,3], Shixiang Zong[1,4], Lili Ren [1,*] and Youqing Luo [1,*]

[1] Beijing Key Laboratory for Forest Pest Control, Beijing Forestry University, Beijing 100083, China;

[2] State Key Laboratory of Woody Oil Resources Utilization, Hunan Academy of Forestry, Changsha 410004, China;

[3] Yuelushan Laboratory, Changsha 410004, China;

[4]State Key Laboratory to Efficient Production of Forest Resources, Beijing Forestry University, Beijing 100083, China

[*] Corresponding author (lily_ren@bjfu.edu.cn)

Abstract: In mixed plantation, Russian olive (*Elaeagnus angustifolia* L.) serves as a "dead-end trap tree" for Asian longhorned beetles (*Anoplophora glabripennis*; ALB), attracting adults to lay eggs, and killing their eggs through gum exudation. Field surveys revealed that ALB preferentially congregates on individual Russian olive trees, with oviposition scars concentrated on 5- to 8-year-old branches, while surrounding trees remain largely uninfested. However, the chemical basis of this dual-level aggregation remains

unclear. Volatiles and key phytohormones (ethylene, abscisic acid, jasmonic acid, and salicylic acid) were profiled in healthy, short-term (August) and long-term (June) ALB-infested Russian olive trees using HS-SPME-GC-MS, GC, and UPLC-MS/MS, revealing distinct chemical signatures associated with infestation duration. Volatile profiles differed markedly in both concentration and composition between healthy trees and those under short- or long-term ALB infestation. These chemical shifts reflected coordinated responses, with clustering patterns driven by the combined effects of multiple volatiles. However, within-tree aggregation was not explained by within-tree VOC variation. Biotic stress was associated with a partial reduction in tree ethylene levels, accompanied by decreased levels of JA and SA, and an abnormal increase in ABA level. Therefore, we hypothesize that the abnormal accumulation of ABA under biotic stress may act as a potential "decoy" signal. Under resource-limited conditions, the suppression of the JA/SA pathway collectively may restructure endogenous defense signals in plants and be associated with disrupted external volatile communication, potentially triggering the ecological phenomenon that “infested plants are more susceptible to ALB infestation”.

Keywords: *Anoplophora glabripennis*; *Elaeagnus angustifolia* L.; dead-end trap tree; HIPVs; phytohormones

Key messages

ALB preferentially aggregates on Russian olive, especially 5–8-year-old branches.

Infested trees emit VOC profiles distinct from healthy trees.

Re-infestation is linked to ABA accumulation and reduced JA/SA.

VOC and hormone shifts may explain “infested plants more susceptible”.

Russian olive shows potential as a dead-end trap tree for ALB.

Introduction

The Asian longhorned beetle (ALB), *Anoplophora glabripennis* (Coleoptera: Cerambycidae), is a widespread and destructive wood-boring pest in China, especially in China's Three-North region. It was included in the list of dangerous forest pests, classified as a Level II forest pest. and also a significant global forest quarantine pest (China National Forestry and Grassland Administration 2013; China National Forestry and Grassland Administration 2019; Wang et al. 2023) . Current control still relies heavily on chemical insecticides and sanitary removal, which are costly and often insufficient once populations are established. Sustainable ALB management therefore requires new, ecologically based control strategies.

The Russian olive (*Elaeagnus angustifolia* L.) exhibits strong adaptability, with relatively low demands on soil, temperature, and humidity. It is native to Eastern Europe and Asia, and is widely distributed across China's Northwest, North, and Northeast regions. Field surveys revealed that the number of oviposition scars chewed by ALB on Russian olive far exceeded that on resistant tree species. These scars are primarily congregated on a single Russian olive, with scars predominatly concentrated on 5- to 8-year-old branches, while surrounding trees remain largely uninfested, demonstrating a pronounced attraction of Russian olive to ALB adults.

Further surveys showed that ALB larvae often died from gum secretion after hatching within the branches, suggesting Russian olive possesses a dual function of attracting adult ALBs to lay their eggs, and eliminating their offspring, consistent with the core characteristics of a "dead-end trap tree". Mixed planting Russian olive and resistant species in specific ratios can prevent infestations from escalating into full-scale outbreaks (Luo 2005; Wang et al. 2023). However, due to limited understanding of “dead-end trap tree”, particularly the disparity in perceptions regarding their attraction and killing functions, they have not been applied in previous pest control efforts (Zhang et al. 1995; Li 2001; Tian et al. 2003; Luo 2005) .

Herbivores rely on volatile organic compounds (VOCs) released by host plants for host location. Females select suitable host plants for larvae based on VOCs, while males determine mating sites through volatiles released by infested plants. Herbivores rely on host plant volatiles for host location and mate selection, but for ALB, host location relies on synergistic interactions between plant volatiles and pheromones. Additionally, induced volatiles released by plants under biotic stress attract predators while regulating defense responses in neighboring plants (Kessler and Baldwin 2001; Thaler et al. 2001; Kessler and Halitschke 2007). For ALB, host location relies on synergistic interactions between plant volatiles and pheromones. The male-produced aggregation pheromone attracts females, and its combination with host volatiles enhances trapping effect (Zhang et al. 2002; Nehme et al. 2009). Sesquiterpenes may play a key role in host location and mate selection (Xu and Teale 2021), and ALB’s host recognition integrates multiple chemical signals rather than a single compound (Lyu et al. 2023). Plant defense against herbivores is regulated by an endogenous

hormone network including JA, SA, ET, and ABA, which exhibits dynamic changes in response to infestation and may jointly drive shifts in plant defense strategies (Rieske and Raffa 1995; Gheysen and Mitchum 2019; Li et al. 2021; Lin et al. 2022; Jamin et al. 2024).

However, it remains unclear whether such defense shifts in Russian olive are associated with ALB aggregation, and whether these shifts vary with infestation duration or host age. To address these questions, we conducted four separate experiments, from the perspective of behavioral preferences, host selection, differences in branch ages and chemical signal regulation.

Our experiment primarily focuses on how Russian olive lures the ALB and induces mass aggregation. As pest outbreaks occur, trees suffer from continuous or repeated stress, leading to fundamental shifts in their defense strategies. We hypothesized that repeated herbivory alters Russian olive VOC profiles and defense-hormone balance, thereby increasing beetle aggregation and plant susceptibility. Through these experiments, we aim to test this hypothesis and determine whether changes in volatile and hormones are associated with ALB aggregation, providing relevant evidence to understand the chemical signatures underlying the shift from resistance to susceptibility in Russian olive.

Materials and methods

Experimental site and design

To evaluate the causes of aggregation behavior of *Anoplophora glabripennis* (ALB) on Russian olive trees, four independent experiments were conducted, focusing on host preference, distribution of scars on branches of different ages, and variations in VOCs and

phytohormones.

The experiments were conducted in Jiayuguan, Gansu, China. The sampling site of host preference assay was selected along Tank Road in Jiayuguan (39.7795°N, 98.2512°E), Gansu Province. Oviposition scar survey and the samples for volatile and phytohormone analysis were conducted in and collected from "First Pier of the Great Wall" in Jiayuguan City, Gansu Province.

Host preference assay (mark–release–recapture)

Observe the behavioral activities of the ALB among Russian olive and Boll's poplar (*Populus alba* var. *pyramidalis* Bunge). A sampling site was selected along Tank Road in Jiayuguan (39.7795°N, 98.2512°E). The site consists of Russian olive, Boll's poplar, and a small number of Mongolian Scotch pine (*Pinus sylvestris* var. *mongholica* Litv.). A release platform was established at the center of the plot. The beetles were sourced from Tank Road, and the supplement beetles were captured near Black Mountain Lake (39.7856°N, 98.1494°E). Beetles were marked by attaching differently colored strings to their pronotum and each ALB was released on the center of the platform, where they were allowed to move freely (Fig. 1). Ten marked beetles were released. After one hour, beetles were recaptured when possible. Marked individuals were monitored further after observed, while unmarked ones were re-tagged and released. Additional marked beetles were supplemented based on field observations. If no marked beetles were observed, two were released each hour, and the process was repeated. A total of 116 ALB (sex ratio approximately 1:1) were released and tagged, with continuous observation conducted for 11 days. 66 had been recaptured at least

once, giving a recapture rate of 56.90%. Record the tree species initially selected by each ALB after released on the platform, and record behavioral activities each hour, including rest, crawling, supplement nutrition, mating and chewing oviposition scars. All observed behaviours (both initial selection and subsequent activities) were included in the statistical analysis.

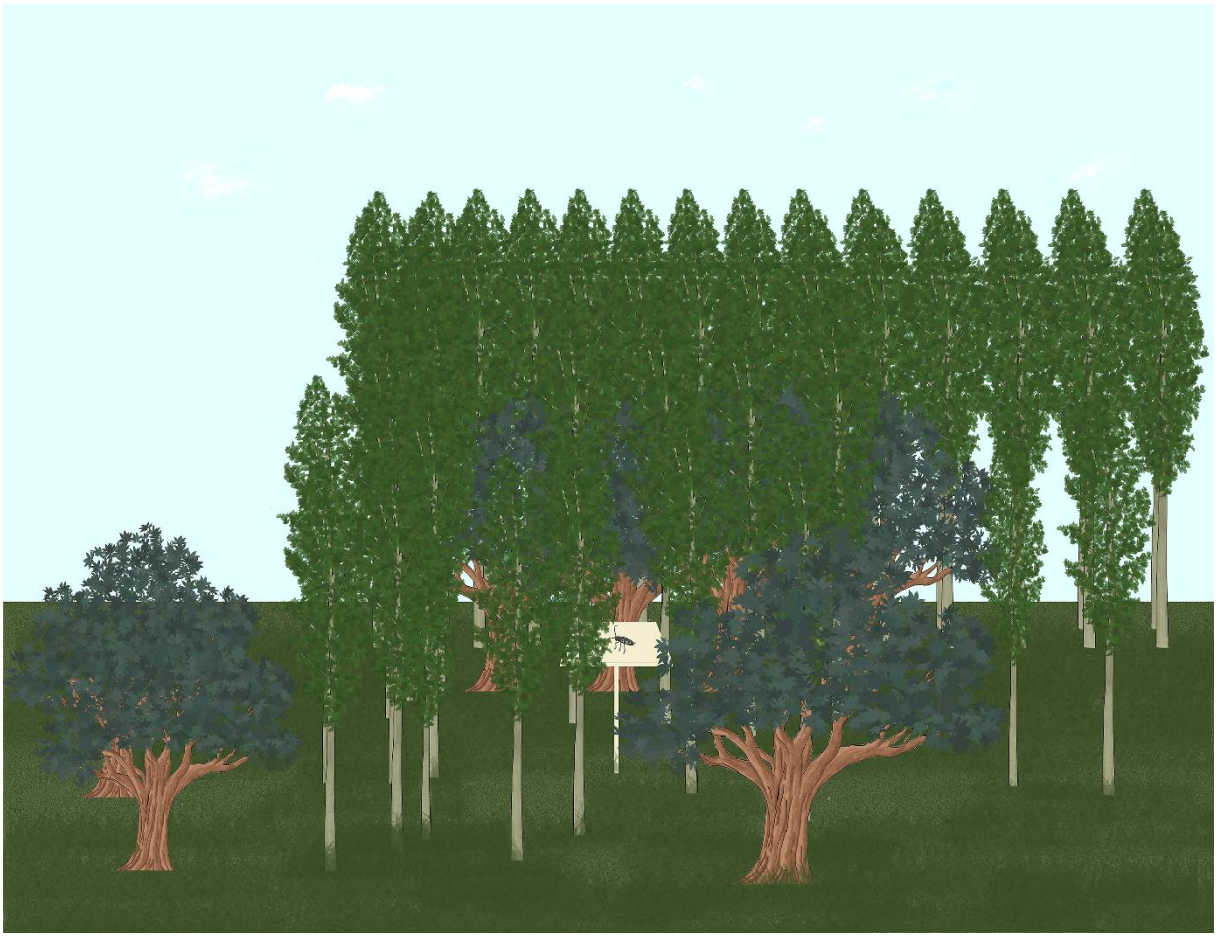


Fig. 1 Schematic diagram of host preference assay site, featuring Boll’s poplar and Russian olive. The release platform is situated at the center, and the pink and blue strings on the pronotum are used to mark different individuals for behavioral observation

Oviposition scar survey across branch age classes

We conducted a field survey of the distribution of ALB oviposition scars on Russian olive's branches of different ages at the sampling site. We selected 20 Russian olive trees with uniform tree height (5.13m±0.12) but varying branch ages as sample trees at "First Pier of the Great Wall" (39.7485°N, 98.2209°E) in Jiayuguan City, Gansu Province. Record the number and location of ALB oviposition scars on each tree, documented a total of 1602 scars and analysed the relationship between scars distribution and branch age. A sampling method was employed to investigate the population density of ALB within the plot, and the number of beetles on branches of different ages was statistically analysed.

Sample collection and treatment classification

To analyse the differences in the induction of VOCs and plant hormones in branches at different stages of infestation and of varying branch ages, samples were collected at the "First Pier of the Great Wall" in Jiayuguan, Gansu Province. A total of 10 healthy trees and 10 infested trees were selected from the field and classified according to diameter at breast height and the number of branches. Branches and leaves from healthy and infested Russian olive were categorized into ＞8-year-old branches of healthy tree (H1), 7- to 8-year-old branches of healthy tree (H2), 5- to 6-year-old branches of healthy tree (H3), ＜5-year-old branches of healthy tree (H4), small branches and leaves of healthy tree (HB), ＞8-year-old branches of infested tree (D1), 7- to 8-year-old branches of infested tree (D2), 5- to 6-year-old branches of infested tree (D3), ＜5-year-old branches of infested tree (D4), and small branches and leaves of infested tree (DB) based on branch age (<5a, 5-6a, 7-8a, >8a). The infested tree showed clear signs of previous oviposition scars, indicating that the trees were under long-term ALB

infestation. In August, field surveys were conducted again at the same trees to obtain the number of new scars formed this year on 10 infested trees (newly infested). Fresh oviposition scars formed during the year were observed on the original 10 infested trees. Samples were collected from all 20 trees. Bark was collected down to the xylem, immediately placed in liquid nitrogen containers, and stored at −80°C for later use. VOCs and plant hormone levels were analysed in the collected samples. As the period from June to August is characterised by both seasonal variety and the number of wounds on infested trees, the time effect and the duration of damage effect cannot be separated in this study.

In this study, repeated sampling was conducted in June and August on the same set of healthy trees (n=10) and infested trees (n=10). This design constitutes both seasonal variety and the number of oviposition on infested trees, but the two factors are not entirely independent.

Volatile organic compound analysis

Weigh 0.5 g each of bark samples from five different branch-age sections of the Russian olive (n=10 trees per treatment, a total 50 groups), chop them into pieces, and place them in sealed 20 mL headspace vials (Agilent, USA) for analysis.This study employed a GCMS QP2010 (Shimadzu, Japan); 50/30 μm DVB/CAR/PDMS SPME fiber (Supelco, USA),and SPME manual injection handle (Supelco, USA).

Headspace Solid-Phase Microextraction

Extraction Head Aging: Using a 50/30 μm DVB/CAR/PDMS SPME fiber, place the fiber at

250°C for 0.5 hours. Remove the fiber and prepare for sample extraction.

Sample extraction: Incubate headspace vials containing samples at 60°C for 45 minutes. Insert the SPME fiber into the headspace vial containing the sample. After 20 minutes of extraction, insert the fiber into the GC inlet at 250°C for 1 minute desorption, then prepare for mass spectrometry detection.

GC-MS Analysis Conditions

GC Conditions: Carrier gas: helium; flow rate: 1.0 $mL \cdot min^{-1}$; splitless injection mode; injection port temperature: 250°C. Temperature program: Hold at 35°C for 3 min, increase at $2°C \cdot min^{-1}$ to 160°C, then ramp at $10°C \cdot min^{-1}$ to 240°C, hold for 9 min.

MS Conditions: Electron ionization (EI) source, electron energy 70 eV, source temperature 280°C, mass transfer line 280°C, mass scan range 30–500 amu; solvent delay time 5 min.

Compound identification and semi-quantification

Integration was performed using the GCMS Solution software, which was used to detect the mass spectral peaks in the raw data, followed by identification of the peaks using the software, matching the mass spectral data to the NIST database (>90%) and then identifying the metabolites on the basis of the match scores. Quantitative analysis was performed by compound peak area, supplemented by qualitative analysis and literature for reference. The relative percentage content of a particular compound was obtained by dividing its relative mass by the total relative mass of all compounds.

The tested compounds were searched by NIST spectral library, supplemented by

literature reports for reference. The relative VOC content was calculated using the peak area normalization method and expressed as the ratio of the peak area of each component to the total peak area. Identification and quantification of compounds were performed through comparison to the mass spectra of NIST 17 library spectra.

Phytohormone analysis

Ethylene quantification by headspace GC

For the gaseous plant hormone ethylene, weigh 1.5 g bark samples (accurate to 0.01 g, n=10, per treatment) into a 20 mL headspace vial (Agilent,USA) for 24h at 28℃ and extract 0.5 mL into a gas chromatograph (Agilent 7890A, USA) equipped with a flame-ionization detector (GC-FID). The injection temperature was 150℃ with a split ratio of 5:1. The chromatographic column was HP-PLOT Q column (30 m × 0.53 mm,40 μm). The column temperature hold at 35°C, increase at 4°C·min^{-1} to 64°C. The carrier gas is nitrogen and the column flow rate is 2 mL·min^{-1}. Ethylene concentration was quantified using the external standard method.

ABA, JA, and SA quantification by UPLC-MS/MS

Different parts of the bark and twigs of Russian olive were ground into a fine powder under liquid nitrogen.Weigh 50 mg accurately, add 0.5 mL isopropanol: water: hydrochloric acid (volume ratio 2:1:0.002). Simultaneously add 10 ng each of isotopically labeled hormones $^{2}H_{6}$-ABA、H_{2}-JA and $^{2}H_{4}$-SA as internal standards. Mix thoroughly and shake at 100 rpm on a 4°C shaker for 30 min. Then add 1 mL of dichloromethane and continue

shaking for 30 min, centrifuge at 13,000 g for 5 min, collect the lower layer, evaporate to dryness under nitrogen, dissolve the sample in 0.1 mL methanol, centrifuge at 13,000 g for 5 min, and proceed with UPLC-MS/MS analysis using the supernatant. Agilent 1260 Infinity UPLC (Agilent，USA) combined with an AB QTRAP 5500 mass spectrometer (AB SCIEX,USA) was applied for quantitative analysis. Liquid chromatographic separation was achieved on an Agilent ZORBAX Eclipse Plus C18 (2.1x100 mm,3.5μm)，employing 0.1% formic acid-water (A) and acetonitrile (B) as mobile phases. The column temperature was maintained at 35℃，and the injection volume was 2 μL. The flow rate was set at 0.3 $ml \cdot min^{-1}$ with the gradient elution. Mass spectrometry analysis utilized an electrospray ionization source operating in negative ion MRM mode. The ion source voltage was adjusted to -4500 V, with the temperature maintained at 600℃. The curtain gas (CUR) pressure was set at 30 psi, the nebulizing gas pressure was 40 psi, and the auxiliary heating gas was 50 psi. Data were processed using Analyst software.

Data analysis

All analyses were performed using SPSS Statistics 26.

A chi-squared test was used to compare the observed distribution of behavioral events with the expected distribution weighted by crown area. The total crown areas of Russian olive (7 trees) and Boll's poplar (49 trees) were measured, yielding a ratio of 0.404 : 0.596. The analysis was performed using SPSS software, with a significance level of $\alpha = 0.05$.

For VOC data, normality was assessed using the Shapiro-Wilk test. As the data did not follow a normal distribution ($P<0.05$), non-parametric methods were employed for subsequent

analysis. Multi-group comparisons were performed using the Kruskal-Wallis H test, followed by Dunn's test for post-hoc pairwise comparisons. To control the false discovery rate in multiple comparisons, the Benjamini-Hochberg FDR correction was applied with q=0.05.

Principal component analysis (PCA) was performed based on the relative abundances of all detected VOCs. The data were automatically Z-score standardized by SPSS through the correlation matrix. To test the statistical significance of group separation, PERMANOVA was conducted based on Bray-Curtis distance with 9,999 permutations, and $P < 0.05$ was considered statistically significant.

For phytohormones, normality of the data was assessed using the Shapiro-Wilk test. Based on the normality test results, three strategies were adopted for between-group comparisons: when the majority of variables (>50%) deviated from normality, the Mann-Whitney U test was uniformly applied to all variables. When a minority of variables (<50%) deviated from normality, normally distributed variables were analyzed using the independent-samples t-test (with Levene's test for homogeneity of variances and adjusted results for unequal variances), while non-normally distributed variables were analyzed using the Mann-Whitney U test. When all variables followed a normal distribution, the t-test was uniformly applied. A P-value < 0.05 was considered statistically significant. All analyses were performed using SPSS.

The correlations among plant hormones (ABA, JA, SA, ET) were assessed by calculating Spearman correlation coefficients and performed using OriginPro 2022 to generate a correlation matrix plot. To control for Type I error due to multiple comparisons, Bonferroni correction was applied, with adjusted significance level set at $\alpha = 0.05 / 6 = 0.0083$.

Results

ALB behavioral events occurred disproportionately on Russian olive

In a mix plantation of Boll's poplar and Russian olive (49:7), a total of 116 ALBs (sex ratio approximately 1:1) were marked and released. Continuous observation over 11 days recorded 296 instances of beetle behavior (Fig. 2), including initial selection and subsequent activities like rest, crawling, supplement, mating, chewing an oviposition scar.

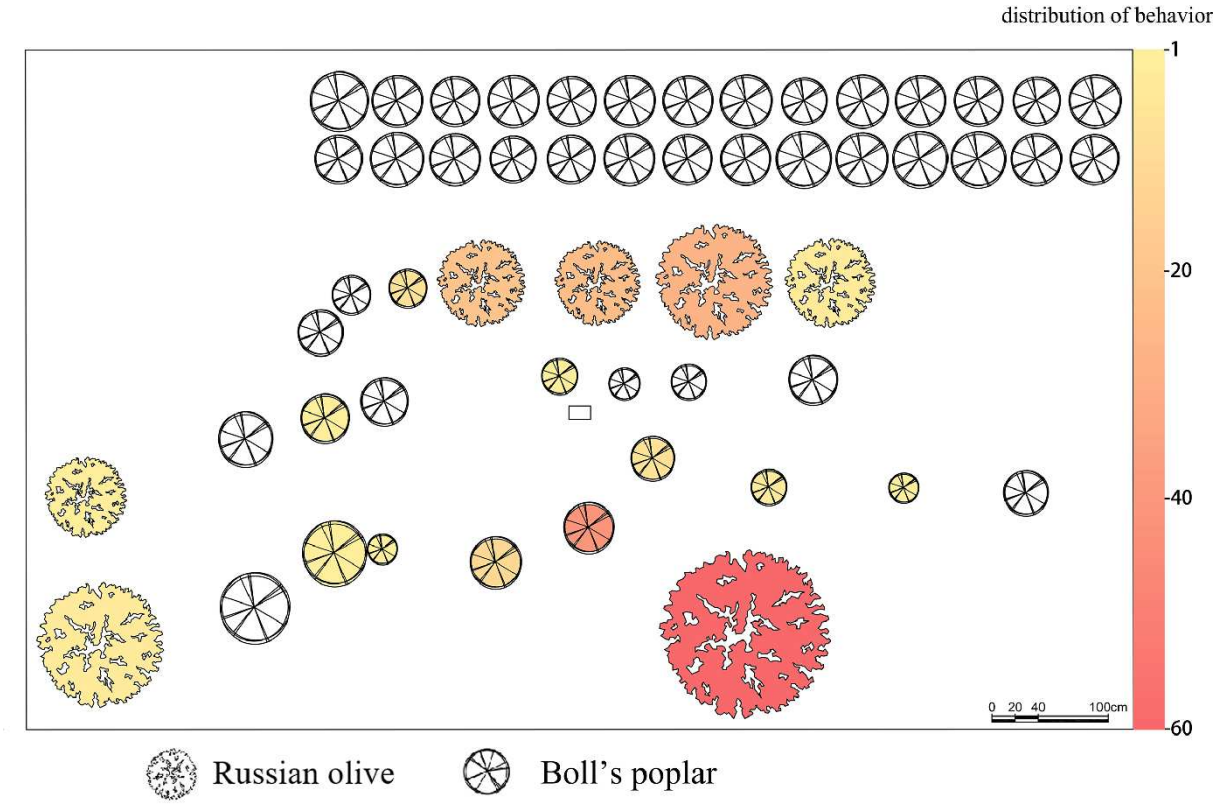


Fig. 2 Preferential selection of the ALB's behavioral distribution heat map. Tree dimensions in the heat map were measured according to actual crown width, with color gradients representing the number of ALB's behavioral distributions

The observed beetles accounted for 56.03% of the total marked beetles. The overall behaviour observation rate was 5.10%, representing the proportion of recorded behavioral events relative to the total potential observable events, calculated as the product of the number of marked beetles and the number of observation sessions. Of all the actually recorded behaviors, 64.44% occurring during rest periods. Behaviors recorded after the initial release (excluding the initial release choice) observed on Russian olive accounted for 32.77% (4.68% per tree), Boll's poplar 16.89% (0.34% per tree), and other locations 11.15% of the total 296 recorded behaviors (including initial release choices) (Fig. 3). The total number of behavioral occurrences of ALB on Russian olive trees was 137, and on Boll's poplars was 77 (including initial selection and subsequent activities, with 40 and 27 instances of initial selection respectively, and the observed ratio was approximately 1.78:1), which deviated significantly from the expected distribution based on the proportion of trees (1:7, $\chi^2 = 519.31$, df = 1, $P < 0.0001$), indicating a significant preference for Russian olive.

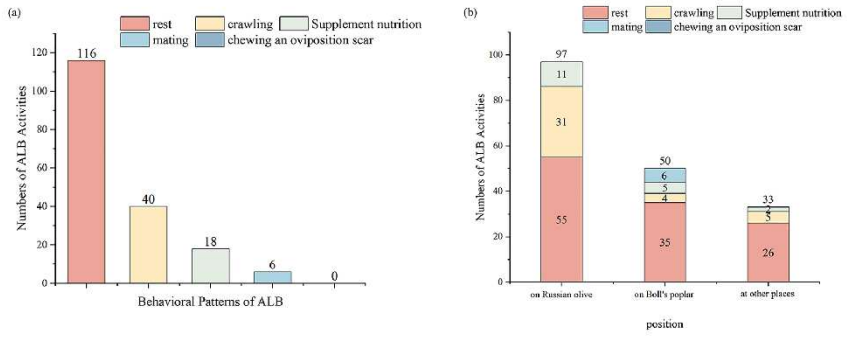


Fig. 3 The behavioural patterns and distribution of ALB within the plot. The plot contained 49 Boll's poplars and 7 Russian olives. A total of 116 Asian longhorned beetles were observed. (a) Numbers of different behavioral patterns of the ALB were observed on Russian olive. (b)

Number of behavioral instances of the ALB at different locations

ALB oviposition scars were concentrated on 5- to 8-year-old branches of Russian olive.

The ALB exhibits distinct preferences for branches of different ages on Russian olive. Due to deviations from normal distribution (Shapiro-Wilk test, $P < 0.05$), the Kruskal-Wallis H test was employed to compare the number of scars chewed on branches of varying ages. A highly significant difference in the number of scars chewed on branches of varying ages (Kruskal-Wallis $H = 25.585$, $df = 3$, $P < 0.001$). Mean rank values showed that 5-6a (mean rank=58.28)> 7-8a (46.40) > <5a (33.90) > >8a (23.43) (Fig. 4). Overall, the number of scars on branches of different ages shows a trend of increasing initially and then decreasing. The oviposition scars chewed by ALB were congregated on 5-8a branches on Russian olive.

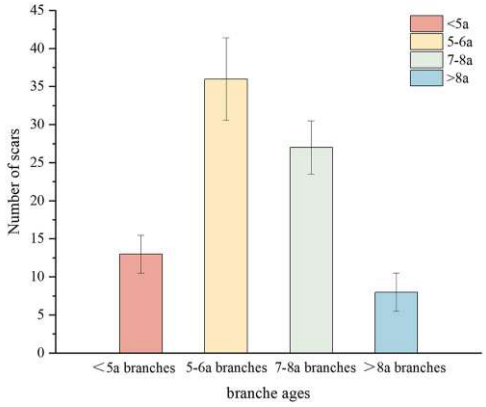


Fig. 4 Distribution of ALB oviposition scars on Russian olive branches of different ages. Branches were classified into 4 groups according to diameter at breast height and the number of branches and categorized into <5, 5-6, 7-8, and >8a. A total of 20 Russian olive trees of uniform height (5.13m±0.12) were selected. Data are expressed as means ± SE

Volatile profiles diverged between healthy and infested trees

Overall volatile composition and PCA separation.

We categorized healthy and infested Russian olive branches and leaves into H1, H2, H3, H4, HB, D1, D2, D3, D4, and DB based on their growth stages: small branches and leaves, <5a, 5-6a, 7-8a and >8a. Through comprehensive analysis, a total of 132 volatiles were detected in June and 95 volatiles were detected in August. We generated heatmaps for June and August showing significantly different volatile metabolites in healthy and infested parts (Fig. 5) .

73 substances were detected in healthy tree species that were prior to new infestation, including alkenes, ketones, alcohols, aldehydes, alkanes, esters, and furans.In previously infested trees, 115 substances were detected, including alkenes, ketones, esters, aldehydes, alkanes, naphthalenes, alcohols, acids, furans, and nitriles (Fig. 5a).

66 substances were detected in healthy tree species that were newly infested, including alkenes, ketones, alcohols, esters, aldehydes, alkanes, ethers, and furans. While in newly infested tree species, 80 substances were detected, including alkenes, ketones, alcohols, esters, aldehydes, alkanes, and furans (Fig. 5b).

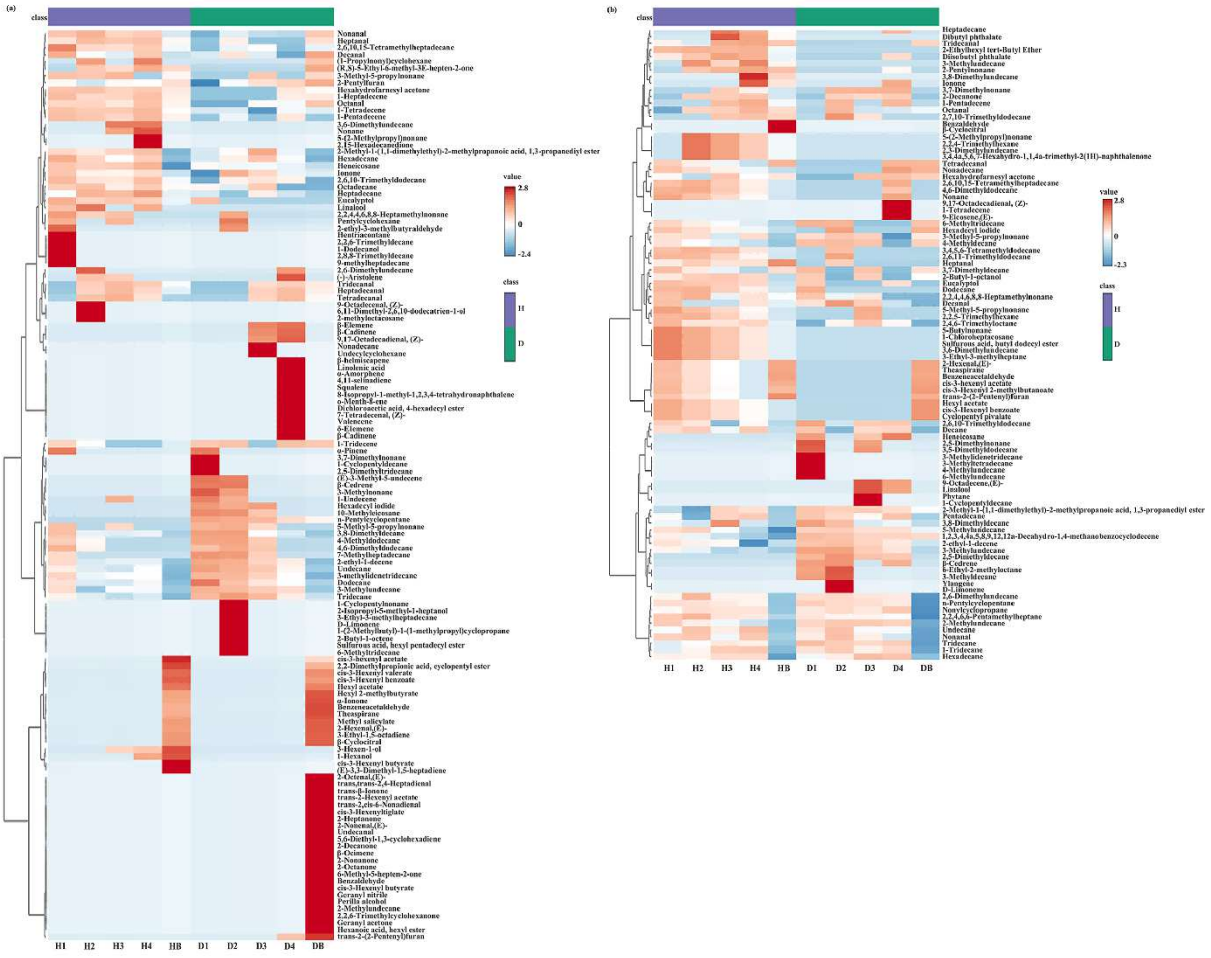


Fig. 5 Heatmaps of volatile metabolites released by healthy and infested Russian olive across different parts before newly infested (a) and after newly infested (b). The branches and leaves were classified into five groups (<5 years, 5-6 years, 7-8 years, >8 years, and small branches and leaves). Samples from healthy trees were labelled H1–H4 and HB, while samples from infested trees were labelled D1–D4 and DB, n=10. The data were normalized and presented as heatmaps. The colors in the heatmaps represent the relative content of volatile compounds

The PCA results showed that PC1 and PC2 account for 20.08% and 11.58% of the total variance. The 95% confidence interval ellipses showed that the ellipses for the four groups are separated from each other. In June, the previously infested trees (6D) clustered on the far right,

whereas the healthy trees (6H) were located centrally along the PC1 axis but lower along the PC2 axis. In August, the healthy trees (8H) were positioned in the mid left region, while the newly infested trees (8D) formed a distinct cluster in the upper left region. All infested trees (6D and 8D) were positioned vertically above their corresponding healthy trees (6H and 8H) along the PC2 axis. These distinct spatial distributions indicate clear differences in VOC profiles due to both sampling time and infestation status (Fig. 6). PERMANOVA further confirmed that there were highly significant differences in the VOC profiles between the four groups (Pseudo-F = 12.256, R^2 = 0.505, p = 0.001).

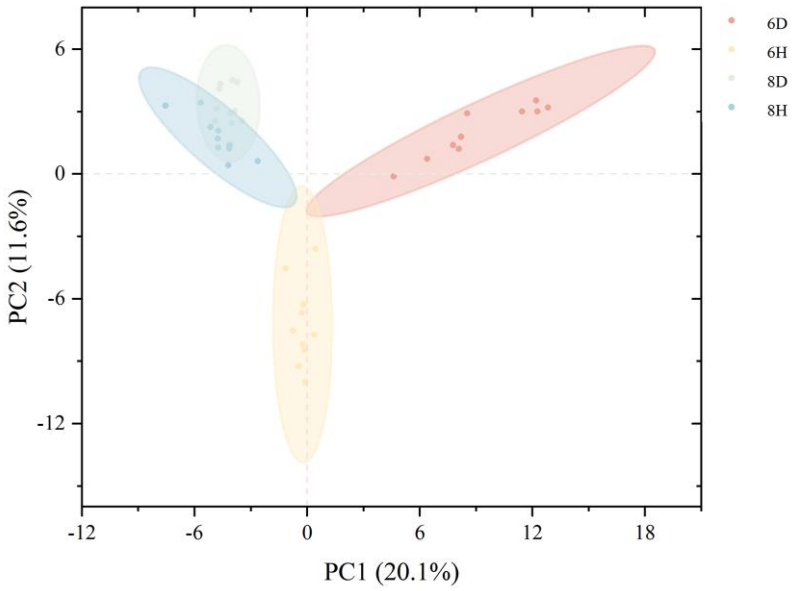


Fig. 6 Principal component analysis (PCA) score plot of plant volatiles grouped by infestation status (H: healthy, D: damaged) and stages (6: June, 8: August). Data were automatically Z-score standardized by SPSS through the correlation matrix. PC1 and PC2 explained 20.08% and 11.58% of the total variance. Ellipses represent 95% confidence intervals for each group. The data were analysed after being normalized, n=10

Key compounds differing between healthy and previously infested trees

Compared to 6H, the levels of Tridecane, 2-ethyl-1-decene and 7-Methylheptadecane detected in 6D showed a significant increase. However, 1-Pentadecene, 2,6,10,15-Tetramethylheptadecane, cis-3-hexenyl acetate, Eucalyptol, Heptanal, Hexahydrofarnesyl acetone and Nonanal showed significant decreases (Table S1).

17 volatile compounds detected only above the identification threshold under the present analytical conditions in 6H. Among these, linalool (5.69%), 3-hexen-1-ol (4.88%), and 1-hexanol (1.61%) exhibited relatively high relative abundance.While 59 volatile compounds were detected only above the identification threshold under the present analytical conditions in 6D, primarily consisting of alkanes, alkenes, and aldehydes. Among these, β-Cedrene (1.43%), 2-Octanone (1.06%), and Geranyl nitrile (0.99%) exhibited higher relative abundance (Table S1).

Significant differences in volatile between previously and newly infested plants

Compared to 6D, 2,6-Dimethylundecane, 2-Methyl-1-(1,1-dimethylethyl)-2-methylpropanoic acid, 1,3-propanediyl ester, 3,7-Dimethylnonane， 6-Methyltridecane, cis-3-hexenyl acetate and Nonanal showed significant increases in 8D (Table S1). 1-Tetradecene， 2-Pentylfuran, 3-methylidenetridecane, 5-Methyl-5-propylnonane, Benzeneacetaldehyde, Dodecane ， Heptadecane, Ionone, trans-2-(2-Pentenyl)furan and Undecane showed significant decreases in 8D.

We detected 32 volatile compounds detected only above the identification threshold under the present analytical conditions in 8D, primarily consisting of alkanes, alkenes, and

alcohols. Among these, pentadecane (9.51%), 2,2,4,6,6-pentamethylheptane (7.88%), linalool (5.15%), and 5-methylundecane (1.02%) exhibited relatively high relative abundance (Table S1).

Key compounds differing between previously and newly infested trees

Compared to 6H, 1-Tridecene, 2,6-Dimethylundecane, 2-Hexenal, (E)-, and 4,6-Dimethyldodecane showed significant increases in 8H (Table S1). 5-Methyl-5-propylnonane, Dodecane, Hexahydrofarnesyl acetone showed significant decreases in 8H.

We detected 31 compounds present detected only above the identification threshold under the present analytical conditions in 8H, primarily alkanes and esters. Among these, 2,2,4,6,6-Pentamethylheptane (20.28%), Pentadecane (6.50%), Benzaldehyde (1.95%), 2-Decanone (1.18%), Decane (1.08%), and 3,7-Dimethylnonane (1.08%) exhibited relatively high relative abundance (Table S1).

Undifferentiated emission of volatiles across tissues regardless of herbivore feeding sites

VOCs were detected in different parts of the Russian olive. Select substances in 5- to 6-year-old branches and 7- to 8-year-old branches (scars-accumulation sections) with similar VOC level ratios that were not significantly different, but exhibited specific differences compared to other sections. After screening and analysis, no VOCs meeting the requirements were identified (Table S2).

Infestation status and sampling stage were associated with phytohormone shifts across branch age classes.

Re-infestation reduced ethylene in oviposition-concentrated branches.

Changes in ethylene content were primarily observed in infested plants. Previously infested Russian olive exhibited higher ethylene levels, with a significant difference were found in <5-year-old branches, while no significant differences were found in other parts. In August, after re-infested ethylene levels in the 5- to 6-year-old branches and 7- to 8-year-old branches (scars-accumulation sections) were significantly lower than that in healthy plants, while no significant differences were detected in other parts. Overall, ethylene levels in most parts of the plant were lower in August than in June, while a moderate seasonal decline was also noted in plants. (Fig. 7).

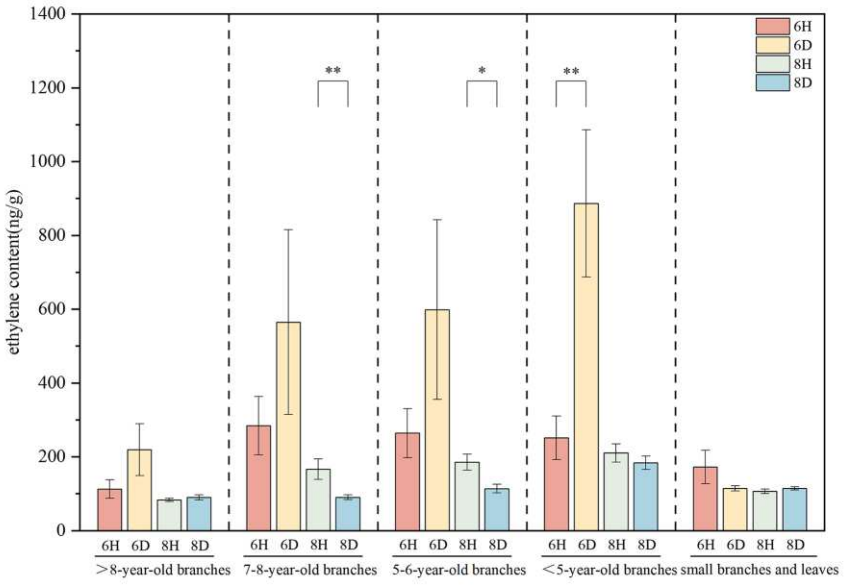


Fig. 7 Ethylene levels released by healthy and infested Russian olive at different stages. Data are expressed as means ± SE, n=10. Independent samples t-test was employed to assess

differences between healthy and infested individuals.* indicates a $P < 0.05$, ** indicates a $P < 0.01$, while*** indicates a $P < 0.001$ (6H:healthy Russian olive in previously infested conditions. 6D: previously infested Russian olive. 8H:healthy Russian olive in newly infested conditions. 8D:newly infested Russian olive)

Re-infestation was associated with a shift from localized to systemic ABA accumulation.

Infestation generally induced ABA accumulation in Russian olive. ABA levels in 5- to 6-year-old branches, 7- to 8-year-old branches (scars-accumulation sections) of previously infested Russian olive were significantly higher than in healthy plants. While ABA levels in other parts were lower than or comparable to that in healthy plants. After re-infestation, ABA levels in all parts of infested Russian olive was extremely significantly higher than that in healthy plants (Fig. 8).

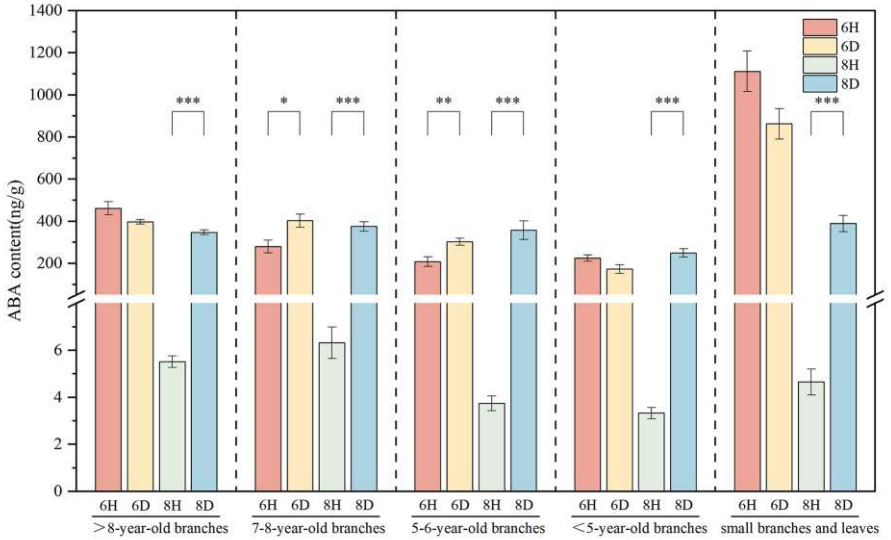
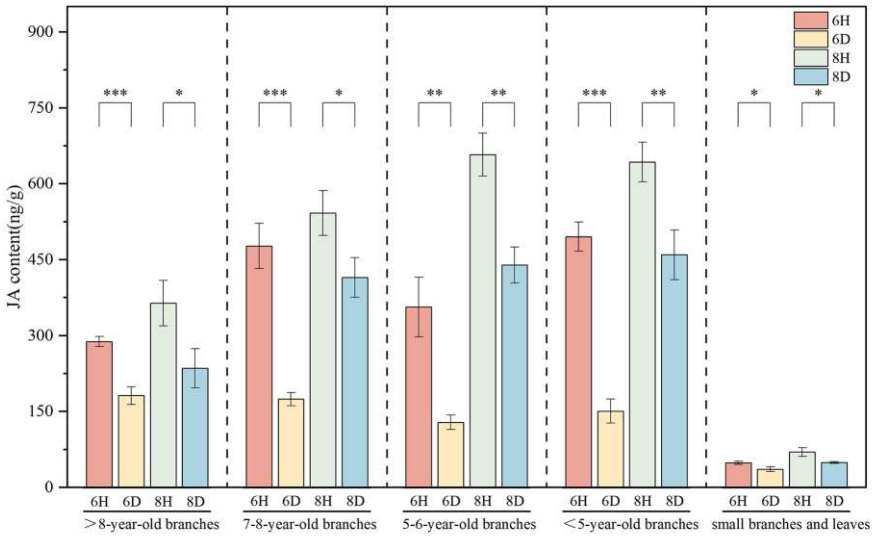


Fig. 8 ABA levels released by healthy and infested Russian olive at different stages. Data are

444 expressed as means ± SE, n=10. Independent samples t-test was employed to assess
445 differences between healthy and infested individuals.* indicates a $P < 0.05$, ** indicates a $P <$
446 0.01, while*** indicates a $P < 0.001$ (6H:healthy Russian olive in previously infested
447 conditions. 6D: previously infested Russian olive. 8H:healthy Russian olive in newly infested
448 conditions. 8D:newly infested Russian olive)
449
450 *JA and SA declined in infested trees regardless of infestation duration*
451 JA and SA levels in different parts of infested Russian olive were significantly lower
452 than those in healthy trees and this difference was consistent across all parts. For JA, highly
453 significant differences ($P < 0.001$) were found in <5-year-old, 7- to 8-year-old
454 and >8-year-old branches in June. Very significant differences ($P < 0.01$) were found in 5- to
455 6-year-old branches in both June and August, and in <5-year-old branches in August. JA level
456 in newly infested Russian olive in August was higher than that in previously infested trees
457 (Fig. 9). For SA, highly significant differences ($P < 0.001$) were observed in 7- to 8-year-old
458 branches in June. Very significant differences ($P < 0.01$) were observed in 5- to 6-year-old
459 branches in both June and August, and in 7- to 8-year-old branches in August (Fig. 10).
460



461

462 **Fig. 9** JA levels released by healthy and infested Russian olive at different stages. Data are
463 expressed as means ± SE, n=10. Independent samples t-test was employed to assess
464 differences between healthy and infested individuals.* indicates a $P < 0.05$, ** indicates a $P <$
465 0.01, while*** indicates a $P < 0.001$ (6H:healthy Russian olive in previously infested
466 conditions. 6D: previously infested Russian olive. 8H:healthy Russian olive in newly infested
467 conditions. 8D:newly infested Russian olive)

468

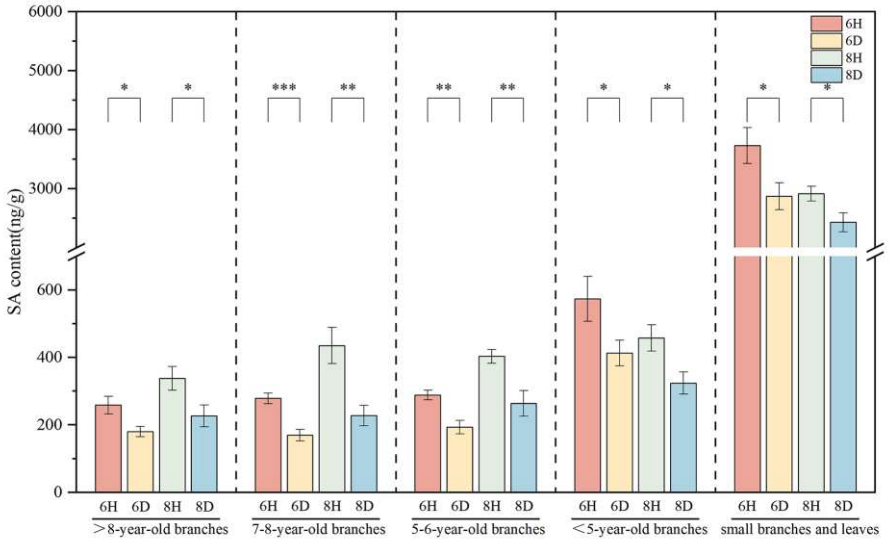


Fig. 10 SA content released by healthy and infested Russian olive at different stages. Data are expressed as means ± SE, n=10. Independent samples t-test was employed to assess differences between healthy and infested individuals.* indicates a $P < 0.05$, ** indicates a $P < 0.01$, while*** indicates a $P < 0.001$ (6H:healthy Russian olive in previously infested conditions. 6D: previously infested Russian olive. 8H:healthy Russian olive in newly infested conditions. 8D:newly infested Russian olive)

Infestation altered phytohormone correlation patterns

A Spearman correlation analysis was performed on the four treatment groups (6D, 6H, 8D, 8H), and multiple comparisons were corrected using the Bonferroni method ($\alpha = 0.05 / 6 = 0.0083$). The results showed that none of the correlations between the hormones reached the adjusted significance level. Nevertheless, the direction and magnitude of the correlation coefficients varied considerably across treatment groups.

Among four treatment groups, the JA's correlation pattern with SA showed the most

prominent change: it was weakly negative in 6D (r=-0.212, n=10, P=0.556; 95%CI[-0.74,0.48]; Bonferroni-adjusted P=1.000), but shifted to a strong positive correlation in 8D (r=0.697, n=10, P=0.03; 95%CI[0.12,0.92]; Bonferroni-adjusted P=0.15).

ET also showed certain pattern variations: its correlation with SA shifted from weakly negative in 6D (r = -0.467, n = 10, P = 0.174; 95% CI [-0.85,0.23]; Bonferroni-adjusted P = 1.000) to moderately positive in 8D (r = 0.418, n = 10, P = 0.229; 95% CI [-0.29,0.83]; Bonferroni-adjusted P = 1.000).

ABA's correlation pattern with JA and SA showed certain pattern variations, shifting from positive correlation in 6D (r=0.394, n=10, P=0.26; 95%CI[-0.31,0.82]; Bonferroni-adjusted P=1.00 and r=0.515, n=10, P=0.13; 95%CI[-0.17,0.86]; Bonferroni-adjusted P=0.77, respectively) to negative correlation in 8D (r=-0.248, n=10, P=0.49; 95%CI[-0.76,0.45]; Bonferroni-adjusted P=1.00 and r=-0.309, n=10, P=0.39; 95%CI-0.79,0.40]; Bonferroni-adjusted P=1.00, respectively). (Fig. 11).

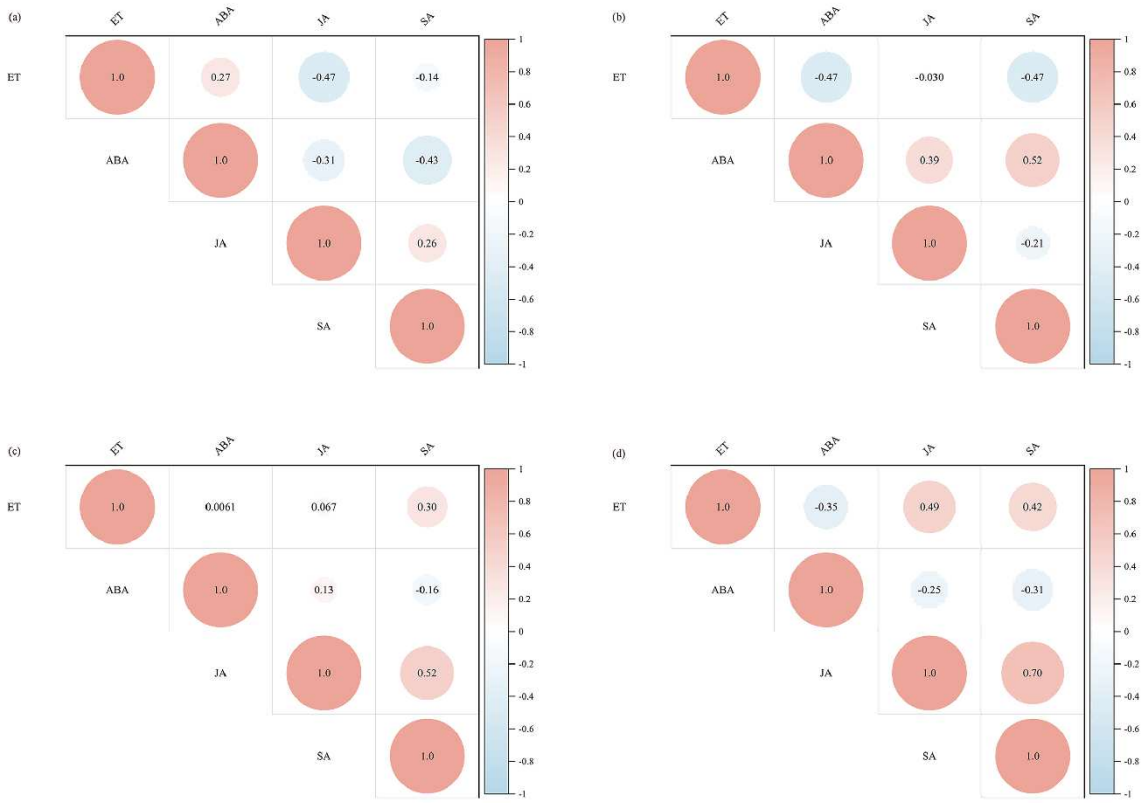


Fig. 11 Correlation matrix of plant hormones (ABA, JA, SA, ET) in different stages, n=10. (**a**) Correlation matrix of plant hormones in healthy Russian olive in June. (**b**) Correlation matrix of plant hormones in infested Russian olive in June (previously infested). (**c**) Correlation matrix of plant hormones in healthy Russian olive in August. (**d**) Correlation matrix of plant hormones in infested Russian olive in August (newly infested). Spearman correlation coefficients are shown in each cell. No statistically significant correlations were detected among the tested variables ($P > 0.05$ for all pairwise comparisons)

Discussion

The potential of Russian olive as a dead-end trap tree for ALB

ALB exhibited a significant oviposition preference for Russian olive and concentrated on

5- to 8-year-old branches. Previous studies have shown that, whilst Russian olive is highly attractive to adult ALBs, the larvae are unable to complete their full development (Li et al. 2024). In summary, the Russian olive possesses the fundamental characteristics of a "dead-end trap tree" for ALB management, attracting adults whilst preventing offspring survival.

Herbivore-Induced alteration of volatiles: An airborne cue for a vulnerable host

Plants typically communicate by releasing volatiles, influencing metabolism, plant phenotypes, gene expression, responses to stress, and the behavioral choices of the receiver organisms (Loreto and D' Auria 2022). The PCA analysis revealed a clear separation among the treatment groups. While previously infested trees deviated toward the right, newly infested trees formed a distinct cluster on the upper left, indicating that long-term infestation and re-infestation induce fundamentally different shifts in VOC profiles.

This rightward deviation in previously infested trees was primarily driven by a functional reversal in VOC profiles. In previously infested Russian olive, levels of attractant compounds such as benzaldehyde, β-Elemene, and various alkanes and alkenes, which had been demonstrated as attractant signals (Obata et al. 1981; Faria and Zanella 2015; Miao et al. 2020), were significantly elevated, and their volatiles had been reconfigured into potential attractant-related signals (Feng et al. 2022; Lv et al. 2024; Zhang et al. 2025). By contrast, healthy Russian olives are rich in compounds with repellent or insecticidal activity, (e.g., eucalyptol, 1-dodecanol), which can interfere with insect pheromone recognition or inhibit their growth and development (Klocke et al. 1987; Tabanca et al. 2014; Wang et al. 2016;

532 Liao et al. 2024).

533 Therefore, the functional difference between infested trees, which release attractant
534 signals, and healthy trees, which release repellent signals, may explain the selective
535 aggregation of pests among trees.

536

537 *Volatile dynamics of Elaeagnus angustifolia under short-term biotic stress.*

538 Infested Russian olive trees can induce neighboring healthy plants to trigger defense
539 priming by releasing HIPVs (Erb 2018; Yao et al. 2023), manifested as the restructuring of
540 volatiles and the accumulation of multiple defense compounds. The synergistic effects of
541 specific compounds, such as the repellent activity observed in combinations of
542 2-butyl-1-octanol with nonanal and 1-dodecene, highlight the central role of compound
543 synergism in chemical defense (Liao et al. 2024). The newly induced decane and significantly
544 elevated (E)-2-hexenal, both known broad-spectrum defense compounds (Zarbin et al. 2000;
545 Skoczek et al. 2017), further suggest that healthy trees activate their defense systems by
546 receiving pest signals. At the same time, the significant decline in certain volatiles in healthy
547 plants in August may reflect a metabolic trade-off (Züst and Agrawal 2017).

548

549 *VOC shifts in re-infested trees.*

550 Compared to previously infested trees, the newly infested trees exhibited a significant
551 difference in their volatile profiles, indicating a shift from a defensive response to tissue
552 breakdown. These newly infested trees exhibited significant surge in pentadecane, diisobutyl
553 phthalate, α-farnesene, with rising levels of nonanal and cis-3-hexenyl acetate. These VOC

554 shifts may attract a variety of insects (Sun et al. 2010; Zong et al. 2013; Mitra et al. 2020;
555 Wang et al. 2020; Feng et al. 2022), potentially trapping weakened trees in a vicious cycle
556 where “infested plants become more susceptible to infestation”. At the same time, the
557 significant decline in certain substances (such as dodecane, heptadecanal and undecane) in
558 newly infested plants may indicate the depletion of defence resources due to sustained feeding
559 (Züst and Agrawal 2017). However, whether ALB is attracted to these volatile compounds
560 remains speculative and requires verification through behavioural experiments. Nevertheless,
561 the continuous release of these “collapse signals” suggest that weakened trees may be more
562 susceptible to the ALB.

563 Linalool was detected in both healthy trees in previously infested conditions and newly
564 infested Russian olives. It typically exhibited insecticidal activity (McCallum et al. 2011;
565 Boachon et al. 2015), but when mixed with specific volatile compounds in certain proportions,
566 it can act as an attractant (Nehme et al. 2010; Ding et al. 2015). We hypothesize that, linalool
567 may independently repel ALB in healthy trees in previously infested conditions, whereas in
568 newly infested trees, it act in combination with other signals to attract ALB at specific ratios.
569 However, the above speculation awaits validation, as Y-tube olfactometer assays, field lure
570 trapping, and GC-EAD analyses were not performed in this study.

571

572 *Integrated function of volatiles: Synergistic action of volatiles from different parts mediates*
573 *insect behavioral selection.*

574 Volatiles serve as host-locating signals to attract ALB, with their effects depend on
575 synergistic interactions among multiple components (Gebreziher and Nakamuta 2016).

Therefore, we conclude that ALB aggregation results from the combined effects of multiple volatiles. However, no significant differences were observed in the volatiles from different parts of the same tree, which fails to explain the branch-level aggregation preference of ALB.This suggests that the aggregation preferences of ALB at the tree level (host tree selection) and its oviposition site selection at the branch level may be governed by different mechanisms. Preferences at the host tree level may rely on differences of volatile compound profiles between healthy and infested plants. In contrast, preferences at the branch level cannot be explained by spatial heterogeneity in volatiles and are likely mediated by internal endogenous factors.

Infestation-associated shifts in phytohormone balance.

Changes in ethylene emission under repeated infestation.

In newly infested plants, ethylene levels in severely damaged parts were lower than in healthy plants, which differed from some reported early stress responses (Kendall and Bjostad 1990; Rieske and Raffa 1995), indicating that long-term or recurring stress may induce negative feedback regulation of ethylene signaling.

Under short-term stress, ethylene positively correlated with SA ($r = 0.418$), indicating a potential cooperative interaction. However, under long-term stress, ethylene levels remained persistently low in severely damaged parts, and shifted to a negative trend with SA ($r = -0.467$). This dynamic shift suggests that the function of ET may shift from cooperation to antagonism as stress duration increases.

The dual role of ABA in plant-herbivore interactions: Partial accumulation and systemic suppression.

The role of ABA in plant defense may be complex (Xiao et al. 2017; Tan et al. 2019; Waadt et al. 2022). Research showed that aphid feeding significantly increased ABA levels in *Arabidopsis* leaves, and prefer wild-type plants rather than *aba1-1* (ABA synthesis-deficient) mutant, which indicates that reduced accumulation of ABA leads to a decrease in the accumulation of defense compounds (Hillwig et al. 2016). Aphid infestation in *Medicago truncatula* upregulates the ABA signaling pathway, triggering stomatal closure and reducing leaf transpiration, thereby improving the host plant's water status and promoting feeding (Sun et al. 2015). In the rice-migratory nematode interaction, ABA suppress JA-induced defense, indicating that the two are negatively correlated (Nahar et al. 2012).

Under pest infestation conditions, the accumulation pattern and function of ABA exhibited a fundamental shift. After previous infestation, ABA levels were significantly increased in severely damaged parts, acting as a partial stress-related signal. However, after re-infestation, ABA remained persistently elevated across all monitored parts, evolving into a "potential systemic ABA-associated defense imbalance".

Further correlation analysis revealed that, under long-term stress, ABA showed positive correlation trends with both JA ($r = 0.394$) and SA ($r = 0.515$), while JA and SA exhibited a negative correlation trend ($r = -0.212$). This pattern suggests that although JA and SA simultaneously decline with the sustained rise in ABA, their correlation with ABA remains positive, implying a precise resource allocation under prolonged stress.

Persistent pest stress drives trees into vulnerable resource-limited states. Abnormally

accumulated ABA may interfere with JA and SA defense pathways, weakening the tree's resistance to subsequent insect attacks. This creates a vicious cycle where “infested plants become more susceptible to infestation” (Pieterse et al. 2009; Vos et al. 2015).

Transformation in JA and SA relations: From dynamic antagonism to constrained defense state.

The JA pathway primarily responds to necrotrophic pathogens and herbivores, while the SA pathway is generally induced by biotrophic and hemi-biotrophic pathogens (Loake and Grant 2007; Pieterse et al. 2012; Wasternack and Hause 2013). Russian olives can activate their defenses by sensing HIPV released by neighboring infested trees. This typically manifests as the systemic accumulation of JA and SA, activating defense priming that influences the host preference of ALB.

It is noteworthy that JA and SA levels in both previously and newly infested plants ultimately remained lower than those in healthy plants, contradicting the commonly reported pattern that “herbivore-induced elevation of defense hormone levels” (Erb et al. 2012). We hypothesize that persistent insect attack depletes substantial plant resources, leading to reduced synthesis JA and SA and its downstream defense capabilities.

As the stress persisted, the relationship between JA and SA shifted from a strong positive correlation under short-term stress ($r = 0.697$) to a weak negative correlation under long-term stress ($r = -0.212$). After newly infestation, both JA and SA pathways are activated in response to biotic stress. However, under long-term stress, the relationship has shifted from synergy to mild antagonism, reflecting a transition toward more precise resource allocation. Combined

with the pronounced accumulation of ABA, the weakening of JA-SA antagonism under long-term stress may indicate an adaptive shift. This suggests that plants shift from broad-spectrum defense toward precision regulation to maintain a constrained defense state under resource-limited conditions.

Physiological consequences of long-term stress: The transformation from "active alert" to "passive decline".

Previously infested Russian olive became chronically vulnerable due to sustained stress. Consequently, their defense mechanisms failed to respond effectively upon re-infestation, contrary to the classic concept of "systemic acquired resistance" or "priming effect" (Conrath et al. 2015; Yang et al. 2022). This reveals the double-edged sword effect of stress memory: when stress exceeds a certain threshold, the memory effect shifts from inducing resistance to resistance decline. This aligns with observations in trees where "accumulated stress leads to growth decline" (Kenneth et al. 2008).

This study links endogenous hormone signaling networks with exogenous volatile profiles, outlining a potential mechanism for Russian olives' vicious cycle of "infested plants becoming more susceptible to infestation". "Internal signaling imbalance" and "external chemical signature" collectively characterize a state of susceptibility. However, this mechanism is currently inferred primarily on field-based correlational evidence, and a causal relationship has not been established. It should be noted that none of the correlations in this section reached statistical significance after Bonferroni correction, and the sample size was small (n = 10), limiting the statistical power. Therefore, the numerical patterns observed here

should be regarded as exploratory findings, and the related inferences warrant further validation with larger sample sizes. Future research could conduct causal tests of the “decoy hypothesis” through exogenous application of ABA or ABA inhibitors, as well as time-course experiments. As a dead-end trap tree, identifying the specific physiological state (e.g., elevated ABA) and vulnerable branch age classes (5- to 8-year-old branches) of Russian olive provides practical targets for optimizing its deployment and developing green pest control technologies based on "attract and kill" strategies.

Author contribution

X.Z. conceived and designed the study, performed the experiments, analysed the data, and wrote the manuscript. Y.L. assisted with sample collection. C.L. provided guidance on experimental design for field surveys. M.L., J.L., and S.Z. reviewed the manuscript. L.R. and Y.L. contributed to supervision and manuscript revision. All authors read and approved the manuscript.

Supplementary material Supplementary material is available in the online version of this article.

Acknowledgements We thank the associate professor Junqi Zhang at the Lab of Plant Biotechnology & Gas Chromatography, Research Center for Analysis & Measurement, Beijing Forestry University, for his generous guidance on experimental operation and design.

Funding This work was supported by National Natural Science Foundation of China [32371886]; National Key Research and Development Program of China [2022YFD1401000]; and the Fundamental Research Funds for the Central Universities [BFUKF202507].

Data Availability Data will be made available upon reasonable request.

Declaration

Conflict of interest The authors declare no conflicts of interest.

Reference

Boachon, B., R. R. Junker, L. Miesch, J.-E. Bassard, R. Höfer, R. Caillieaudeaux, D. E. Seidel, A. Lesot, C. Heinrich, J.-F. Ginglinger, L. Allouche, B. Vincent, D. S. C. Wahyuni, C. Paetz, F. Beran, M. Miesch, B. Schneider, K. Leiss and D. Werck-Reichhart (2015). "CYP76C1 (Cytochrome P450)-Mediated Linalool Metabolism and the Formation of Volatile and Soluble Linalool Oxides in Arabidopsis Flowers: A Strategy for Defense against Floral Antagonists." Plant Cell 27: 2972-2990. https://doi.org/10.1105/tpc.15.00399

China National Forestry and Grassland Administration (2013). National List of Dangerous Pests in Forestry. C. N. F. a. G. Administration. Beijing. https://www.gov.cn/gzdt//att/att/site1/20130115/782bcb888c4d125f076501.pdf

China National Forestry and Grassland Administration (2019). National Forestry and Grassland Administration Announcement (No. 20 of 2019) (National Forestry Pest Census). C.

N. F. a. G. Administration. Beijing: 4. https://www.forestry.gov.cn/c/www/gkzfwj/272644.jhtml

Conrath, U., G. J. Beckers, C. J. Langenbach and M. R. Jaskiewicz (2015). "Priming for enhanced defense." Annu Rev Phytopathol 53: 97-119. https://doi.org/10.1146/annurev-phyto-080614-120132

Ding, J., Y. Chen, X. Xie, G. Zhu, X. Liu and Q. Liu (2015). "Comparison of Four Different Approaches for the Extraction of *Elaeagnus angustifolia* Flower Volatiles." Plant Sci J 33: 116-125. https://doi.org/10.11913/PSJ.2095-0837.2015.10116

Erb, M. (2018). "Volatiles as inducers and suppressors of plant defense and immunity — origins, specificity, perception and signaling." Curr Opin Plant Biol 44: 117-121. https://doi.org/10.1016/j.pbi.2018.03.008

Erb, M., S. Meldau and G. A. Howe (2012). "Role of phytohormones in insect-specific plant reactions." Trends Plant Sci 17: 250-259. https://doi.org/10.1016/j.tplants.2012.01.003

Faria, L. R. R. and F. C. V. Zanella (2015). "Beta-ionone attracts *Euglossa mandibularis* (Hymenoptera, Apidae) males in western Paraná forests." Rev Bras Entomol 59: 260-264. https://doi.org/10.1016/j.rbe.2015.05.003

Feng, H., C. Gou, D. Aimaiti, P. Sun, L. Wang and H. Hao (2022). "Plant volatile organic compounds attractive to *Lygus pratensis*." Open Life Sci 17: 362-371. https://doi.org/10.1515/biol-2022-0038

727 Gebreziher, H. G. and K. Nakamuta (2016). "Responses of a predatory bug to a mixture of
728 herbivore-induced plant volatiles from multiple plant species." Arthropod-Plant Interact 10:
729 429-444. https://doi.org/10.1007/s11829-016-9456-6
730 Gheysen, G. and M. G. Mitchum (2019). "Phytoparasitic Nematode Control of Plant
731 Hormone Pathways." Plant Physiol 179: 1212-1226. https://doi.org/10.1104/pp.18.01067
732 Hillwig, M. S., M. Chiozza, C. L. Casteel, S. T. Lau, J. Hohenstein, E. Hernández, G. Jander
733 and G. C. MacIntosh (2016). "Abscisic acid deficiency increases defence responses against
734 *Myzus persicae* in Arabidopsis." Mol Plant Pathol 17: 225-235.
735 https://doi.org/10.1111/mpp.12274
736 Jamin, A., T. Adil, I. Tarikul, M. Sajad, M. Mohammad, K. A. Sliacka and C. Rizhao (2024).
737 "Defense strategies and associated phytohormonal regulation in Brassica plants in response to
738 chewing and sap-sucking insects." Front Plant Sci 15: 1376917.
739 https://doi.org/10.3389/fpls.2024.1376917
740 Kendall, D. M. and L. B. Bjostad (1990). "Phytohormone ecology : Herbivory by *Thrips*
741 *tabaci* induces greater ethylene production in intact onions than mechanical damage alone." J
742 Chem Ecol 16: 981-991. https://doi.org/10.1007/bf01016506
743 Kenneth, F. R., H. A. Brian, J. B. Barbara, L. C. Allan, A. H. Jeffrey, G. T. Monica and H. R.
744 William (2008). "Cross-scale Drivers of Natural Disturbances Prone to Anthropogenic
745 Amplification: The Dynamics of Bark Beetle Eruptions." BioScience 58: 501-517.
746 https://doi.org/10.1641/B580607
747 Kessler, A. and I. T. Baldwin (2001). "Defensive function of herbivore-induced plant volatile
748 emissions in nature." Science 291: 2141-2144. https://doi.org/10.1126/science.291.5511.2141

749 Kessler, A. and R. Halitschke (2007). "Specificity and complexity: the impact of
750 herbivore-induced plant responses on arthropod community structure." Curr Opin Plant Biol
751 10: 409-414. https://doi.org/10.1016/j.pbi.2007.06.001
752 Klocke, J. A., M. V. Darlington and M. F. Balandrin (1987). "1,8-Cineole (Eucalyptol), a
753 mosquito feeding and ovipositional repellent from volatile oil of *Hemizonia fitchii*
754 (Asteraceae)." J Chem Ecol 13: 2131-2141. https://doi.org/10.1007/bf01012562
755 Li, C., J. Pei, L. Wang, Y. Tian, L. Ren and Y. Luo (2024). "Interactions at the Oviposition
756 Scar: Molecular and Metabolic Insights into Elaeagnus angustifolia's Resistance Response to
757 Anoplophora glabripennis." Int J Mol Sci 25: 9504. https://doi.org/10.3390/ijms25179504
758 Li, J. (2001) Behavioral responses and mechanism of *Anoplophora glabripennis*
759 (Motschulsky) to host volatile compounds phd dissertation, Beijing Forestry University
760 Li, Y.-M., C. Forney, B. Bondada, F. Leng and Z.-S. Xie (2021). "The Molecular Regulation
761 of Carbon Sink Strength in Grapevine (*Vitis vinifera* L.)." Front Plant Sci 11: 606918.
762 https://doi.org/10.3389/fpls.2020.606918
763 Liao, H., Z. Zhou, Y. Liu, Y. Luo, C. Zhang, Y. Feng, Y. Shu and J. Wang (2024). "'The Three
764 Sisters' (maize/bean/squash) polyculture promotes the direct and indirect defences of maize
765 against herbivores." Eur J Agron 155: 127118. https://doi.org/10.1016/j.eja.2024.127118
766 Lin, P.-A., Y. Chen, G. Ponce, F. E. Acevedo, J. P. Lynch, C. T. Anderson, J. G. Ali and G. W.
767 Felton (2022). "Stomata-mediated interactions between plants, herbivores, and the
768 environment." Trends Plant Sci 27: 287-300. https://doi.org/10.1016/j.tplants.2021.08.017
769 Loake, G. and M. Grant (2007). "Salicylic acid in plant defence—the players and
770 protagonists." Curr Opin Plant Biol 10: 466-472. https://doi.org/10.1016/j.pbi.2007.08.008

771 Loreto, F. and S. D'Auria (2022). "How do plants sense volatiles sent by other plants?"
772 Trends Plant Sci 27: 29-38. https://doi.org/10.1016/j.tplants.2021.08.009
773 Luo, Y. (2005) Theory and techniques of ecological regulation of poplar longhorned beetle
774 disaster in shelter-forest. phd dissertation, Beijing Forestry University
775 Lv, J.-Y., Z.-J. Meng, Y.-N. Deng, C.-W. Zhang, M.-M. Tao and S.-C. Yan (2024). "Active
776 volatile components of the preferred hosts are potential attractants to *Hyphantria cunea*
777 adults." Pestic Biochem Physiol 202: 105910. https://doi.org/10.1016/j.pestbp.2024.105910
778 Lyu, F., X. Hai and Z. Wang (2023). "A Review of the Host Plant Location and Recognition
779 Mechanisms of Asian Longhorn Beetle." Insects 14: 292.
780 https://doi.org/10.3390/insects14030292
781 McCallum, E. J., J. P. Cunningham, J. Lücker, M. P. Zalucki, J. J. De Voss and J. R. Botella
782 (2011). "Increased plant volatile production affects oviposition, but not larval development, in
783 the moth Helicoverpa armigera." J Exp Biol 214: 3672-3677.
784 https://doi.org/10.1242/jeb.059923
785 Miao, C., W. Li, S. Dong, Q. Luo, M. Zhao and X. Guo (2020). "A chemical basis for
786 different oviposition rates of *Helicoverpa assulta* across two *Nicotiana* species."
787 Arthropod-Plant Interact 14: 705-716. https://doi.org/10.1007/s11829-020-09779-0
788 Mitra, P., S. Das and A. Barik (2020). "Leaf waxes from Lathyrus sativus: short-range
789 attractant and stimulant for nymph laying in a viviparous insect." Chemoecology 30: 117-129.
790 https://doi.org/10.1007/s00049-020-00303-7

791 Nahar, K., T. Kyndt, Y. B. Nzogela and G. Gheysen (2012). "Abscisic acid interacts
792 antagonistically with classical defense pathways in rice–migratory nematode interaction."
793 New Phytol 196: 901-913. https://doi.org/10.1111/j.1469-8137.2012.04310.x
794 Nehme, M. E., M. A. Keena, A. Zhang, T. C. Baker and K. Hoover (2009). "Attraction of
795 Anoplophora glabripennis to Male-Produced Pheromone and Plant Volatiles." Environ
796 Entomol 38: 1745-1755. https://doi.org/10.1603/022.038.0628
797 Nehme, M. E., M. A. Keena, A. Zhang, T. C. Baker, Z. Xu and K. Hoover (2010). "Evaluating
798 the use of male-produced pheromone components and plant volatiles in two trap designs to
799 monitor *Anoplophora glabripennis*." Environ Entomol 39: 169-176.
800 https://doi.org/10.1603/en09177
801 Obata, T., M. Kim, H.-S. Koh and H. Fukami (1981). "Planthopper Attractant(s) in the Rice
802 Plant." Jpn. J. Appl. Entomol. Zool. 25: 47-51. https://doi.org/10.1303/jjaez.25.47
803 Pieterse, C. M., A. Leon-Reyes, S. Van der Ent and S. C. Van Wees (2009). "Networking by
804 small-molecule hormones in plant immunity." Nat Chem Biol 5: 308-316.
805 https://doi.org/10.1038/nchembio.164
806 Pieterse, C. M. J., D. Van der Does, C. Zamioudis, A. Leon-Reyes and S. C. M. Van Wees
807 (2012). "Hormonal Modulation of Plant Immunity." Annu Rev Cell Dev Biol 28: 489-521.
808 https://doi.org/10.1146/annurev-cellbio-092910-154055
809 Rieske, L. K. and K. F. Raffa (1995). "Ethylene emission by a deciduous tree,Tilia americana,
810 in response to feeding by introduced basswood thrips, *Thrips calcaratus*." J Chem Ecol 21:
811 187-197. https://doi.org/10.1007/bf02036650

812 Skoczek, A., D. Piesik, A. Wenda-Piesik, B. Buszewski, J. Bocianowski and M. Wawrzyniak
813 (2017). "Volatile organic compounds released by maize following herbivory or insect extract
814 application and communication between plants." J Appl Entomol 141: 630-643.
815 https://doi.org/10.1111/jen.12367
816 Sun, X.-L., G.-C. Wang, X.-M. Cai, S. Jin, Y. Gao and Z.-M. Chen (2010). "The Tea Weevil,
817 Myllocerinus aurolineatus, is Attracted to Volatiles Induced by Conspecifics." J Chem Ecol 36:
818 388-395. https://doi.org/10.1007/s10886-010-9771-9
819 Sun, Y., H. Guo, L. Yuan, J. Wei, W. Zhang and F. Ge (2015). "Plant stomatal closure
820 improves aphid feeding under elevated CO_2." Global Change Biol 21: 2739-2748.
821 https://doi.org/10.1111/gcb.12858
822 Tabanca, N., Z. Gao, B. Demirci, N. Techen, D. E. Wedge, A. Ali, B. J. Sampson, C. Werle, U.
823 R. Bernier, I. A. Khan and K. H. Baser (2014). "Molecular and phytochemical investigation of
824 *Angelica dahurica* and *Angelica pubescentis* essential oils and their biological activity against
825 *Aedes aegypti*, *Stephanitis pyrioides*, and *Colletotrichum* species." J Agric Food Chem 62:
826 8848-8857. https://doi.org/10.1021/jf5024752
827 Tan, L., Q. Liu, Y. Song, G. Zhou, L. Luan, Q. Weng and C. He (2019). "Differential Function
828 of Endogenous and Exogenous Abscisic Acid during Bacterial Pattern-Induced Production of
829 Reactive Oxygen Species in *Arabidopsis*." Int J Mol Sci 20: 2544.
830 https://doi.org/10.3390/ijms20102544
831 Thaler, J. S., M. J. Stout, R. Karban and S. S. Duffey (2001). "Jasmonate-mediated induced
832 plant resistance affects a community of herbivores." Ecol Entomol 26: 312-324.
833 https://doi.org/10.1046/j.1365-2311.2001.00324.x

834 Tian, R., J. Yu and W. Zhao (2003). "Preliminary study on the trapping function of Russian
835 olive for controlling populations of the Asian Longhorn Beetle." J Inn Mong For Sci Technol
836 4: 23-25. https://doi.org/10.3969/j.issn.1007-4066.2003.04.006
837 Vos, I. A., L. Moritz, C. M. Pieterse and S. C. Van Wees (2015). "Impact of hormonal
838 crosstalk on plant resistance and fitness under multi-attacker conditions." Front Plant Sci 6:
839 639. https://doi.org/10.3389/fpls.2015.00639
840 Waadt, R., C. A. Seller, P.-K. Hsu, Y. Takahashi, S. Munemasa and J. I. Schroeder (2022).
841 "Plant hormone regulation of abiotic stress responses." Nat Rev Mol Cell Biol 23: 680-694.
842 https://doi.org/10.1038/s41580-022-00479-6
843 Wang, C., G. Li, C. Miao, M. Zhao, B. Wang and X. Guo (2020). "Nonanal modulates
844 oviposition preference in female *Helicoverpa assulta* (Lepidoptera: Noctuidae) via the
845 activation of peripheral neurons." Pest Manage Sci 76: 3159-3167.
846 https://doi.org/10.1002/ps.5870
847 Wang, F., J. Deng, C. Schal, Y. Lou, G. Zhou, B. Ye, X. Yin, Z. Xu and L. Shen (2016).
848 "Non-Host Plant Volatiles Disrupt Sex Pheromone Communication in a Specialist Herbivore."
849 Sci Rep 6: 32666. https://doi.org/10.1038/srep32666
850 Wang, L., C. Li, Y. Luo, G. Wang, Z. Dou, I. U. I. Haq, S. Shang and M. Cui (2023). "Current
851 and future control of the wood-boring pest *Anoplophora glabripennis*." Insect Sci 30:
852 1534-1551. https://doi.org/10.1111/1744-7917.13187
853 Wasternack, C. and B. Hause (2013). "Jasmonates: biosynthesis, perception, signal
854 transduction and action in plant stress response, growth and development. An update to the

2007 review in Annals of Botany." Ann Bot 111: 1021-1058. https://doi.org/10.1093/aob/mct067

Xiao, X., X. Cheng, K. Yin, H. Li and J.-L. Qiu (2017). "Abscisic acid negatively regulates post-penetration resistance of *Arabidopsis* to the biotrophic powdery mildew fungus." Sci China Life Sci 60: 891-901. https://doi.org/10.1007/s11427-017-9036-2

Xu, T. and S. A. Teale (2021). "Chemical Ecology of the Asian Longhorn Beetle, *Anoplophora glabripennis*." J Chem Ecol 47: 489-503. https://doi.org/10.1007/s10886-021-01280-z

Yang, Z., P. Zhi and C. Chang (2022). "Priming seeds for the future: Plant immune memory and application in crop protection." Front Plant Sci 13: 961840. https://doi.org/10.3389/fpls.2022.961840

Yao, C., L. Du, Q. Liu, X. Hu, W. Ye, T. C. J. Turlings and Y. Li (2023). "Stemborer-induced rice plant volatiles boost direct and indirect resistance in neighboring plants." New Phytol 237: 2375-2387. https://doi.org/10.1111/nph.18548

Zarbin, P. H. G., M. Borges, A. A. dos Santos, A. R. M. de Oliveira, F. Simonelli and F. D. Marques (2000). "Alarm pheromone system of stink bug *Piezodorus guildinii* (Heteroptera: Pentatomidae)." J Braz Chem Soc 11: 424-428. https://doi.org/10.1590/S0103-50532000000400017

Zhang, A., J. E. Oliver, J. R. Aldrich, B. Wang and V. C. Mastro (2002). "Stimulatory Beetle Volatiles for the Asian Longhorned Beetle, *Anoplophora glabripennis* (Motschulsky)." Z Naturforsch C 57: 553-558. https://doi.org/10.1515/znc-2002-5-626

876 Zhang, E., J. Zhou, R. Liu, X. Yang, Z. Bai and Y. Liu (1995). "Survey on Longhorn Beetle
877 damage to Shelterbelts in Ningxia and configuration of stand structure." J Northwest For Coll
878 10: 16-21+39.
879 https://kns.cnki.net/kcms2/article/abstract?v=esvOG1ozB-gYZyifJTVK_AvdKg14n-YZmGD
880 fr9X3keAfP7FvpJ1qIBNxxC1wvAXXOuJ70C0iWAFYE2q-DoqeB57DStzY5s8LS7Xck9Us
881 v8jximf1tqbk4oRl9fbBL6cOMqnzRdNyGGJdWlRl-XuZdxPBf9x2vVkG51zyo9hiLosA5azD
882 NMUy2Q==&uniplatform=NZKPT&language=CHS
883 Zhang, X. Y., W. H. Han, F. A.-O. Zhang, J. X. Wang, S. S. Liu and X. A.-O. Wang (2025).
884 "Attraction of *Nicotiana benthamiana* to *Bemisia tabaci* is related to a chemical signal in
885 plant volatile, undecane." Pest Manage Sci 81: 7359-7369. https://doi.org/10.1002/ps.8411
886 Zong, S., X. Liu, C. Cao and Y. Luo (2013). "Development of Semiochemical Attractants for
887 Monitoring and Controlling Chlorophorus caragana." Z Naturforsch C 68: 243-252.
888 https://doi.org/10.1515/znc-2013-5-611
889 Züst, T. and A. A. Agrawal (2017). "Trade-Offs Between Plant Growth and Defense Against
890 Insect Herbivory: An Emerging Mechanistic Synthesis." Annu Rev Plant Biol 68: 513-534.
891 https://doi.org/10.1146/annurev-arplant-042916-040856
892

Supplementary Files

This is a list of supplementary files associated with this preprint. Click to download.

- TableS1.xlsx
- TableS2.xlsx